MITSUBISHI HEAVY INDUSTRIES, LTD.
16-5, KONAN 2-CHOME, MINATO-KU
TOKYO, JAPAN

May 20, 2009

Document Control Desk
U.S. Nuclear Regulatory Commission
Washington, DC 20555-0001

Attention: Mr. Jeffrey A. Ciocco

Docket No. 52-021
MHI Ref: UAP-HF-09239

Subject: MHI's Responses to NRC's Requests for Additional Information on Advanced Accumulator for US-APWR Topical Report MUAP-07001-P, Revision 2

With this letter, Mitsubishi Heavy Industries, LTD. ("MHI") transmits to the U.S. Nuclear Regulatory Commission ("NRC") the document entitled "MHI's Responses to NRC's Requests for Additional Information on Advanced Accumulator for US-APWR Topical Report MUAP-07001-P, Revision 2" a document package that responds to the NRC's Requests for Additional Information dated April 7, 2009.

As indicated in the enclosed materials, this document contains information that MHI considers proprietary, and therefore should be withheld from public disclosure pursuant to 10 C.F.R. § 2.390 (a)(4) as trade secrets and commercial or financial information which is privileged or confidential. A non-proprietary version of the document is also being submitted with the information identified as proprietary redacted and replaced by the designation "[ ]".

This letter includes a copy of the proprietary version (Enclosure 2), a copy of the non-proprietary version (Enclosure 3), and the Affidavit of Yoshiki Ogata (Enclosure 1) which identifies the reasons MHI respectfully requests that all materials designated as "Proprietary" in Enclosure 2 be withheld from public disclosure pursuant to 10 C.F.R. § 2.390 (a)(4).

Please contact Dr. C. Keith Paulson, Senior Technical Manager, Mitsubishi Nuclear Energy Systems, Inc. if the NRC has questions concerning any aspect of the submittal. His contact information is below.

Sincerely,

Y. Ogata

Yoshiki Ogata,
General Manager- APWR Promoting Department
Mitsubishi Heavy Industries, LTD.

D081
NRO

Enclosures:
1 - Affidavit of Yoshiki Ogata

2 - MHI's Responses to NRC's Requests for Additional Information on Advanced Accumulator for US-APWR Topical Report MUAP-07001-P, Revision 2 (proprietary)

3 - MHI's Responses to NRC's Requests for Additional Information on Advanced Accumulator for US-APWR Topical Report MUAP-07001-P, Revision 2 (non-proprietary)

CC: J. A. Ciocco
C. K. Paulson

Contact Information
C. Keith Paulson, Senior Technical Manager
Mitsubishi Nuclear Energy Systems, Inc.
300 Oxford Drive, Suite 301
Monroeville, PA 15146
E-mail: ckpaulson@mnes-us.com
Telephone: (412) 373-6466

ENCLOSURE 1

Docket No. 52-021
MHI Ref: UAP-HF-09239

MITSUBISHI HEAVY INDUSTRIES, LTD.

AFFIDAVIT

I, Yoshiki Ogata, state as follows:

1. I am General Manager, APWR Promoting Department, of Mitsubishi Heavy Industries, LTD ("MHI"), and have been delegated the function of reviewing MHI's US-APWR documentation to determine whether it contains information that should be withheld from public disclosure pursuant to 10 C.F.R. § 2.390 (a)(4) as trade secrets and commercial or financial information which is privileged or confidential.

2. In accordance with my responsibilities, I have reviewed the enclosed document entitled "MHI's Responses to NRC's Requests for Additional Information on Advanced Accumulator for US-APWR Topical Report MUAP-07001-P, Revision 2" dated May 2009, and have determined that portions of the document contain proprietary information that should be withheld from public disclosure. Those pages containing proprietary information are identified with the label "Proprietary" on the top of the page and the proprietary information has been bracketed with an open and closed bracket as shown here "[ ]". The first page of the document indicates that all information identified as "Proprietary" should be withheld from public disclosure pursuant to 10 C.F.R. § 2.390 (a)(4).

3. The information identified as proprietary in the enclosed document has in the past been, and will continue to be, held in confidence by MHI and its disclosure outside the company is limited to regulatory bodies, customers and potential customers, and their agents, suppliers, and licensees, and others with a legitimate need for the information, and is always subject to suitable measures to protect it from unauthorized use or disclosure.

4. The basis for holding the referenced information confidential is that it describes the unique design of the Advanced Accumulator developed by MHI and not used in the exact form by any of MHI's competitors. This information was developed at significant cost to MHI, since it required the performance of Research and Development and detailed design for its software and hardware extending over several years.

5. The referenced information is being furnished to the Nuclear Regulatory Commission ("NRC") in confidence and solely for the purpose of information to the NRC staff.

6. The referenced information is not available in public sources and could not be gathered readily from other publicly available information. Other than through the provisions in paragraph 3 above, MHI knows of no way the information could be lawfully acquired by organizations or individuals outside of MHI.

7. Public disclosure of the referenced information would assist competitors of MH in their design of new nuclear power plants without incurring the costs or risks associated with the design and testing of the subject systems. Therefore, disclosure of the information contained in the referenced document would have the following negative impacts on the competitive position of MH in the U.S. nuclear plant market:

A. Loss of competitive advantage due to the costs associated with development and testing of the Advanced Accumulator. Providing public access to such information permits competitors to duplicate or mimic the Advanced Accumulator design without incurring the associated costs.

B. Loss of competitive advantage of the US-APWR created by benefits of enhanced plant safety, and reduced operation and maintenance costs associated with the Advanced Accumulator .

I declare under penalty of perjury that the foregoing affidavit and the matters stated therein are true and correct to the best of my knowledge, information and belief.

Executed on this 20th day of May, 2009.

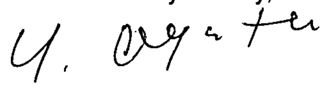

Yoshiki Ogata,
General Manager- APWR Promoting Department

Mitsubishi Heavy Industries, LTD.

Enclosure 3

UAP-HF-09239
Docket No. 52-021

MHI's Responses to NRC's Requests for Additional Information

on

Advanced Accumulator for US-APWAR Topical Report MUAP-07001-P, Revision 2

May 2009
(Non-Proprietary)

RAI 30.

The outlet nozzle throat area and the vortex chamber, during the high flow and the low flow periods, respectively, have low pressure regions. These low pressure regions are susceptible to evolving of dissolved gases and the production of vapor. This gaseous region may lead to increases in friction pressure drop and/or choking.

MHI's response to RAI 13 dated July 20, 2007, stated that it did not provide any detection system to observe cavitation in the ½ scale and 1/5 scale tests, but concluded that there must be some cavitation occurring in the tests. For small flow conditions, it also concluded that there cannot be cavitation at the exit nozzle throat. In its response to RAI 2 dated September 2008, MHI stated that under small flow rate conditions, there can be a stable cavitation cloud at the center of the vortex chamber and the size of the cavitation cloud is scale dependent.

(a) Will there be cavitation in the flow damper outlet nozzle/injection pipe during the large and small flow conditions, respectively? Is the cavitation a vaporous or gaseous (due to the dissolved nitrogen) cavitation? What is the critical cavitation factor when this type of cavitation first occur?

(b) Will there be cavitation in the vortex chamber during small flow conditions? Is the cavitation a vaporous or gaseous cavitation? What is the critical cavitation factor for vortex cavitation?

(c) In the ½ scale model experiments, at what times do you expect cavitation to occur during both the large flow and small flow conditions and where?

Response

(a) We agree that there will be cavitation in the diffuser of the flow damper outlet nozzle for large flow injection.

Cavitation in the diffuser for large flow injection will be vaporous cavitation. Our estimate of the inception cavitation factor is $\sigma_v \approx 8$ for large flow injection where the flow rate coefficient began to reduce as cavitation factor becomes smaller as shown in Fig. 5.1-1 in the topical report.

(b) There will not be cavitation in the diffuser for small flow injection, but may be at the center of the vortex chamber. We speculated it as follows:

There may exist a strong and steady vortex in the chamber so that the pressure at the center must be low enough to generate cavitation there. The strong vortex also forces flow close to the wall of the diffuser downstream the throat, and generates reverse flow at the center of the diffuser. The reverse flow makes the pressure at the throat equivalent to that in the injection pipe which is much higher than the vapor pressure. Thus, the cavitation must be confined upstream of the throat which is the critical cross section of the flow rate. Please, see the location of cavitation calculated by CFD in Response to RAI 53. In other words, cavitation does not affect the critical flow at the throat nor flow rate coefficient. It can also deduce there is no flow choking under the plant operating conditions.

The inception cavitation factor is unknown for small flow injection, because there is no effect of cavitation to the flow rate coefficient.

(c) Please see the response mentioned above.

RAI 31.
How does the cavitation factor calculated with the flow damper outlet conditions represent cavitation in the vortex chamber?

Response
There is no way of representation of cavitation in the vortex chamber based on the cavitation factor defined by Equation (4-1) in the Topical Report MUAP-07001-P(R2). That is because the cavitation factor is used for evaluation of cavitation effect based on the flow rate coefficient, and not for cavitation state in the vortex chamber which does not affect the flow rate coefficient of the flow damper.

RAI 32.

Is there an estimate of void fraction in the vortex chamber and the flow damper outlet nozzle for the large and small flow conditions, respectively? Will the two phases separate and why? What is the effect of the voiding on the flow rate coefficient and any possible flow choking?

Response

For small flow rate, please see the MHI's response to RAI30 of this document. Flow at the throat is single phase and void fraction is estimated as null. There may be cavitation at the center of a strong vortex in the vortex chamber, but the void fraction is unknown. There is no effect of voiding on the flow rate coefficient as mentioned above and no flow choking.

For large flow rate, cavitation occurs in the diffuser where pressure is a minimum due to the curvature of streamlines, or centrifugal force, by gradual expansion of the cross sectional area of the diffuser in addition to high velocity flow from the throat, and will be maintained at the critical pressure, or vapor pressure. Therefore, pressure at the throat must be higher than the critical pressure, and flow will be single phase. Hence, there is no choked flow at the throat. If there were a choked flow in the diffuser, flow rate must be invariant even though pressure difference across the flow damper varies. It will cause inconsistency of flow rate coefficients to each other among different test conditions. This pattern is not observed in the test results, and the test report indicates the data support no choked flow.

RAI 33.

It will take time for accumulator to become saturated with nitrogen. The upper layer will saturate but thereafter, the dissolved gas will diffuse to the rest of the accumulator liquid. If there are any convection currents in the liquid, the mixing will be even faster. The response to RAI 5b dated September 2008, regarding the dissolved ratio of nitrogen in terms of diffusion period of 2 years through 10 years, does provide the actual concentration of the dissolved gas, and the dissolution of the gas as the fluid particles move to the lower pressure. The amount of gas that will evolve depends on the nucleation sites and interfacial area.

Why are the effects of nucleation sites, interfacial area density and convection not addressed, in addition to the diffusion process?

Response

About the effect of convection currents:

Temperature difference between water and the wall can induce convection currents in an accumulator tank. We have no data showing temperature variation in accumulator tanks at operating plants, so we cannot evaluate convection currents affecting on nitrogen dissolution. The maximum effect of dissolved nitrogen on cavitation will be at the saturated condition. That is why we carried out Case 5 with water saturated with nitrogen. If enough nitrogen is supplied, some nitrogen will be dissolved in the water to reach the saturation condition, and excess nitrogen that forms as tiny bubbles in water which may act as cavitation nuclei. If there are too many nuclei, some will combine to form larger bubbles and escape out of water. Therefore, there must be maximum density of cavitation nuclei. Convection currents in an actual accumulator tank may increase dissolution of nitrogen in water, but will not affect the number of cavitation nuclei. In Case 5 Study, bubbling and showering of nitrogen were supplied to water until the pressure in the tank stopped its variation and became sedentary. This case represents the maximum or conservative approach to estimate the number of cavitation nuclei in saturated water in Case 5. Consequently, Case 5 was the critical condition of nitrogen to cavitation.

About nucleation sites and interfacial area density:

Numerous cavitation nuclei are generally contained in water. There are also some cavitation nuclei on the walls of the vortex chamber and the throat. The size of nuclei seems to be in the order of 10^{-3}inch in water.

The pressure drop in the actual accumulator tank is slow. However, let's consider a nitrogen bubble that experiences abrupt depression from the storage pressure of 5.33MPa to an atmospheric pressure of 0.101MPa at time t=0 sec as a stepwise to be able to examine the growth of the bubble as the most conservative. The bubble at first rapidly expands due to gas expansion, then nitrogen slowly permeates in water due to diffusion of saturated nitrogen. Bubble dynamics due to gas expansion in inviscid fluid is given by the following equation (L.D. Landau and E.M. Lifshitz: Fluid Mechanics, Pergamon Press, 1975):

$$P(t) = p_0 + \frac{1}{2}\rho\left[\frac{d^2(R^2)}{dt^2} + \left(\frac{dR}{dt}\right)^2\right] \qquad (33\text{-}1)$$

Where R is radius of the bubble, $P(t)$ pressure on the surface of the bubble, t time, ρ density of fluid, and p_0 ambient pressure.

The distension of a spherical bubble with an initial radius 2×10^{-3}in (0.05mm) due to gas expansion is shown in Figure 33-1. Surface tension on the bubble was taken into account in the calculation. Bubble distension due to gas expansion is very rapid. For adiabatic change, or specific heat ratio γ=1.4, the bubble is distended in 9x10^{-6} sec, and for isothermal change, or γ=1.0, the bubble is distended in 1.6x10^{-5} sec. An actual bubble will be abruptly distended in time between them.

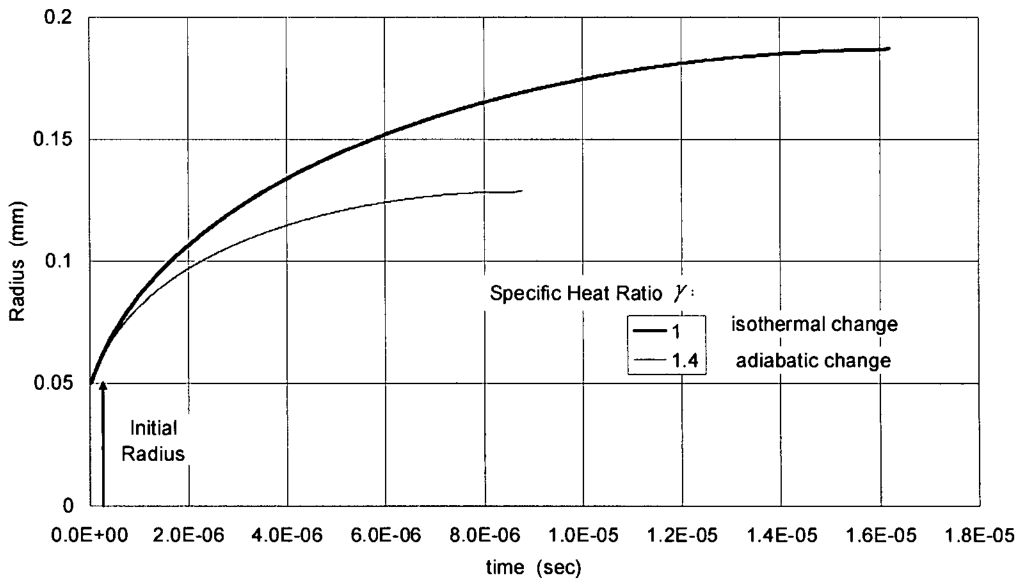

Fig. 33-1 Example of Distension of a Nitrogen Bubble due to Gas Expansion

Nitrogen diffusion affects the growth of a bubble. For simplicity, the solution of one dimensional diffusion of nitrogen in the water around the bubble is shown as

$$c = c_R + (c_\infty - c_R) erf \frac{x}{2\sqrt{Dt}} \qquad (33\text{-}2)$$

where c is concentration of nitrogen, c_R and c_∞ concentrations at radii $r = R$ and $r \to \infty$ respectively, $x = r - R$, D diffusion coefficient of nitrogen in water, and an error function

$$erf\eta = \frac{2}{\sqrt{\pi}} \int_0^\eta \exp(-\xi^2) d\xi . \qquad (33\text{-}3)$$

The distension of the spherical bubble due to nitrogen diffusion after the gas expansion is shown in Figure 33-2.
It is shown that the distension due to the diffusion of nitrogen is very small for about 0.15sec which is the duration a bubble in water passes through the vortex chamber and the throat. The diffusion around a bubble depends on its radius, and it is nonlinear. The diffusion of nitrogen is very slow.

The speed of nitrogen diffusion is the same for nuclei on the walls as for bubbles in water. The former are sedentary on the walls and the bubbles expand to a certain size at which superjacent flow carries them. The growth rate is controlled by slow diffusion of nitrogen in water.

Consequently, effect of nitrogen is the abrupt distension of bubbles, or cavitation nuclei, in the form of gas expansion, and diffusion of nitrogen is negligible.

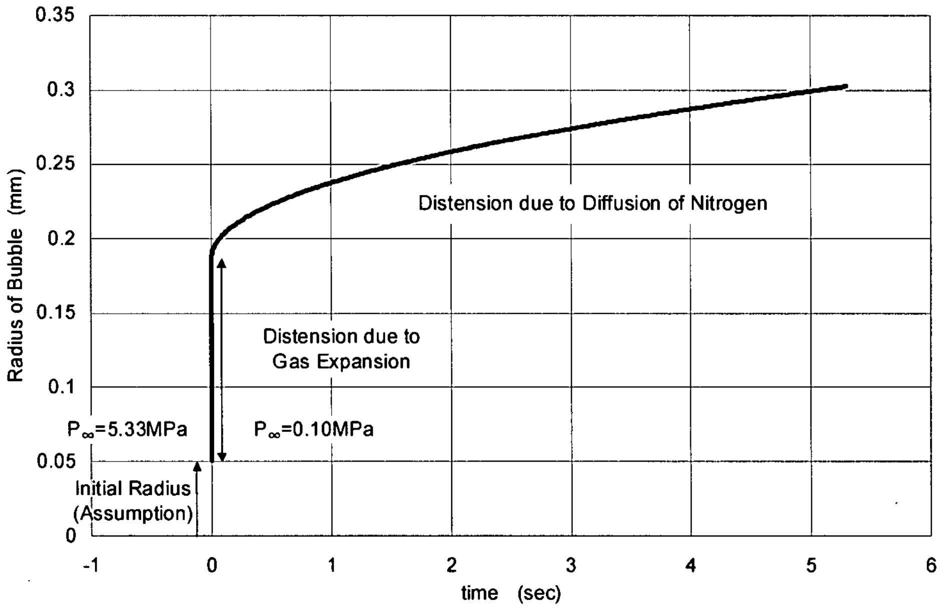

Fig. 33-2 Example of Distension of a Nitrogen Bubble due to Diffusion

RAI 34.

Figure 4.2.4-9 in the topical report (MUAP-07001) compares Case 1 and Case 5 of the ½ scale tests with same accumulator tank and exhaust tank pressures. In Case 5, the liquid was saturated with nitrogen. A comparison of data from two tests indicates that the data for cavitation factor and flow rate coefficient are shifted to lower values for Case 5. In response to RAI 16-B, dated July 20, 2007, on why Case 5 was not included in developing correlations, MHI stated that "using the Case 5 test data will result in evaluating flow rate coefficient smaller than that of the actual accumulator because the test condition in test Case 5 with nitrogen gas compulsorily saturated by bubbling and showering is much more critical than the actual accumulator". However, disregard of Case 5 test result would completely ignore the effect the dissolved nitrogen, though not saturated, in the actual accumulator.

(a) Explain why Case 5 has lower values of the flow rate coefficient and cavitation factor relative to Case 1.

(b) How do the proposed accumulator flow rate characteristic correlations for flow rate coefficient account for dissolved nitrogen?

Response

(a) Please see the response to RAI 33. In the Case 5 test, it seems that the maximum number of cavitation nuclei existed in the nitrogen-saturated water by bubbling and showering. The generation of microbubbles was observed in the tank along the test initiation in the Case 5 test, and this fact supports the above description. The cavitation nuclei seem to grow rapidly due to gas expansion induced by pressure drop, and change effective density of water to increase pressure loss at throat portion. This is the reason for cavitation factor and flow rate coefficient in the Case 5 test being lower than those in the Case 1.

(b) Flow coefficient reduction described in item (a) above is not considered in the proposed accumulator flow rate characteristic correlations. This is because the flow coefficient reduction in the Case 5 test is induced by dissolving nitrogen in test tank water compulsorily by bubbling and showering, and this condition cannot exist in actual accumulator. In addition, it is not expected, as described in the response to RAI 33, that dissolved nitrogen diffusion accelerates the growth of bubbles to increase pressure loss at the outlet of throat portion.

RAI 35.

The results of 1/2 - scale test cases presented in Figures 4.2.4 of topical report MUAP-07001-P, indicate that the flow rate coefficient starts to decrease around cavitation factor of 4 for the large flow phase. The analysis, presented in response to RAI 21 (Sept 2008), is not clear. It assumes that the wall pressure as throat pressure (i.e., Pw = Pt, Eq. 21-2). It is not obvious how pressure at the throat could be equated to pressure along the wall especially when cavitation occurs at the throat. It is also not clear why dp, instead of dt, is used in the term (Pt π/4 dp^2) in Eq. 21-8. The original conservation of momentum projected along the axis of the nozzle is represented by Eq. 21-1, where the first term is Pt π/4 dt^2, not Pt π/4 dp^2.

The critical cavitation factor computed from MHI's analysis, in the responses to RAI 13-B (July 2007) and RAI 21 (Sept 2008), will be too low to have any cavitation during both the large and small flow rate conditions. As such, these derived equations are not helpful to predict cavitation.

Using simple Bernoulli equation with loss coefficient, we can get an equation:

$$\sigma_v = \frac{(P_2 - P_v)}{\zeta_d \rho V_2^2/2} = \frac{(P_t - P_v)}{\zeta_d \rho V_2^2/2} - \frac{\zeta_p}{\zeta_d} + \frac{\left(\left(\frac{d_2}{d_t}\right)^4 - 1\right)}{\zeta_d} \qquad (35\text{-}1)$$

This indicates that the critical cavitations inception for large flow will be around (-1+15/ ζ d), or approximately 2 (since ζ d= ζ p =5 for large flow). Therefore, there will be cavitation for large flow phase. For the small flow, the total loss coefficient, ζ d, is around 250 but the injection pipe loss coefficient ζ p will be close to 5. So the cavitation inception expression will be (-(p/ ζ d) +15/ ζ d). That will imply a critical cavitation factor value of 0.04, which is much smaller than the data (Fig. 5.1-1, MUAP 07001-P).

(a) Explain why the correlation starts to predict a decrease in flow rate coefficient at cavitation parameter around 4.0 for the large flow condition (Figure 5.1-1, MUAP-07001)?

(b) How will this critical cavitation factor of 0.04 explain cavitation in the vortex chamber for the small flow condition as was stated in the MHI's response to RAI 2 of Sept 2008?

Response

$P_w=P_t$ is an assumption which was used as a rough estimation. A more rigorous expression of cavitation factor is Equation (21-9) for which mean pressure coefficient, $\overline{C}_p$, must be given.

d_p is correct in the first term in equation (21-8).

Equation (21-1) is

[ ] (21-1)

Equation (21-6) is

[ ] (21-6)

Equation (21-7) is

[ ] (21-7)

where the diameter of the exit of the diffuser, d_2, is equal to that of the injection pipe, d_p.

Using equations (21-6) and (21-7), the second term on the left hand side of equation (21-1) becomes

[ ] (21-a)

Substituting this equation into the second term of equation (21-1) gives equation (21-8) as

[ ] (21-8)

Namely, the first term on the right hand side of equation (21-a) combines with the first term of equation (21-1) to yield the first term of equation (21-8).

Equation (21-9) cited in the previous Response to RAIs No.2, UAP-HF-08174-P(R0), was derived from the control volume approach, where P_2 is pressure at the exit of the outlet nozzle as shown in Figure 21-1, while P_2 cited in equation (35-1) is pressure at the exit of the injection pipe. It causes the second term on the right hand side of equation (35-1).

[ ] (21-9)

The last term of equation (35-1) is slightly different from that of equation (21-9), which might come from the difference of the assumptions of no pressure loss in the diffuser for equation (35-1) and of pressure distribution on the wall of the diffuser for equation (21-9).

(a) The theoretical value of cavitation factor is relatively close to the experimental value for large flow injection. Also, the pressure at the throat is close to the minimum value in the diffuser. Figure 5.1-1 of the Topical Report indicates degradation of flow rate coefficient for cavitation factor of $\sigma_v \approx 7$ or less for large flow injection. Cavitation might occur around this range. The cavitation factor defines pressure at the exit of the outlet nozzle as the characteristic pressure for the flow damper, not pressure at the exit of the injection pipe.

As mentioned in Response to RAI 32, cavitation may occur in the diffuser where local pressure is a minimum for large flow injection. If cavitation occurs in the diffuser, flow passing through the orifice separates from the wall of the diffuser and forms a vena contracta. Since pressure of the vena contracta is the minimum along the axis of the outlet nozzle of the flow damper and kept close to vapor pressure when cavitation occurs on the wall of the diffuser, the pressure at the throat is higher than the vapor pressure. To keep the pressure of the vena contracta close to vapor pressure causes degradation of flow rate coefficient of the flow damper when flow rate increases.

(b) The cavitation factor of 0.04 is used to evaluate cavitation in the diffuser. We agree that there is no cavitation at the throat or diffuser during small flow injection, but the pressure at the center of the vortex in the chamber is smaller than that at the throat, and it is possible that there is cavitation at the center of the vortex chamber for small flow injection. Please see Response to RAI 53.

RAI 36.

The accumulator characteristic correlations developed with the ½-scale accumulator test data indicate that the cavitation factor and flow rate coefficient are the only groups that represent important phenomena for high and low flow conditions.

(a) Are the cavitation factor and flow rate coefficient the only dimensionless groups that represent the important phenomena?

(b) In MHI's response to RAI 9-A (Sept, 2008), why is there no gravity term in the momentum equation? What are the boundary conditions (configuration)? What is the length scale (D) and the basis for being appropriate for all directions? Eq. 9-2 describes the local momentum balance. The statement below that Eq. states that the pressure loss is only function of Reynolds number. However, there is pressure loss beside the friction (viscous) loss that depends on the geometry. How is the pressure loss based on geometry preserved in different size facilities?

(c) Is the response for RAI 9-B (Sept, 2008) applicable to both large and small flow conditions? In case of gaseous cavitation (dissolved nitrogen), how do you calculate critical cavitation pressure.

(d) In the response to RAI 9-C, how are possible cavitation effects taken into account in the scaling assessment?

Response

The states of flow in the full-height 1/2-scale model of the flow damper and the standpipe are shown in Fig. 36-1. The scale of all dimensions is 1/2 except the height of the standpipe. For large flow injection, the ratio of cross sectional areas of the standpipe and the large flow pipe is[ ]so that there is no flow separation in the elbow between them to make a uniform velocity distribution in the large flow pipe. In other words, the length of the standpipe does not affect the flow in the flow damper. In addition to that, the inlet of the standpipe below the anti-vortex cap is designed to have configuration without flow separation so that flow in the standpipe is uniform. The ratio of cross sectional areas of the accumulator tank and the standpipe is[ ], so the flow toward the inlet of the standpipe is rapidly accelerated for which the accumulator tank serves as a reservoir where water is almost at rest. Consequently, flow at the inlet of the standpipe is not affected by the flow conditions in the accumulator tank but only by the gas pressure. Friction losses in the standpipe for both the actual accumulator and the full-height 1/2 scale model are less than[ ]of the flow damper and negligible. Friction loss in the flow damper was evaluated with the data of 1/5 and 1/2 scale models, and the scale effect to friction loss was confirmed to be negligible for the operating conditions of the advanced accumulator. It is because the length of the flow path in the flow damper is less than that of the standpipe in addition to high Reynolds number.

For flow switching, a water column in the standpipe is in one dimensional motion as in water hammer analysis. Since it has actual velocity, actual amount of undershoot of water level happens in the full-height 1/2-scale standpipe so that simulation of water level transition in the standpipe can be realized. This is the reason the full height standpipe was chosen for the 1/2 scale model.

Froude number was used for the similarity of transition of water level in the standpipe during flow switching. A water column in the standpipe is in one dimensional motion as in water hammer analysis, where the height of the standpipe affects the motion of the water column but the hydraulic diameter does not. Please see the Response to RAI 18, UAP-HF-08174-P(R0). Therefore, the height of the standpipe should be used for the Froude number. The height of the standpipe for the full height 1/2 scale model is the identical as for the actual one.

For small flow injection, flow in the standpipe stops, so flow in the flow damper of 1/2 scale model is similar to that in the actual one. At very last stage of small flow injection, water level in the accumulator tank approaches the small flow pipe after the safety injection pumps start and the accumulator tank ends its role.

The minimum cross sectional area of the flow path is at the throat of the outlet nozzle. The cross sectional areas of the standpipe and the accumulator tank are[ ]and[ ]times the minimum cross sectional area respectively. Their dynamic pressures are less than[ ]of that at the throat and negligibly small. Consequently, the flow resistance of the advanced accumulator can be determined by the flow resistance of the flow damper.

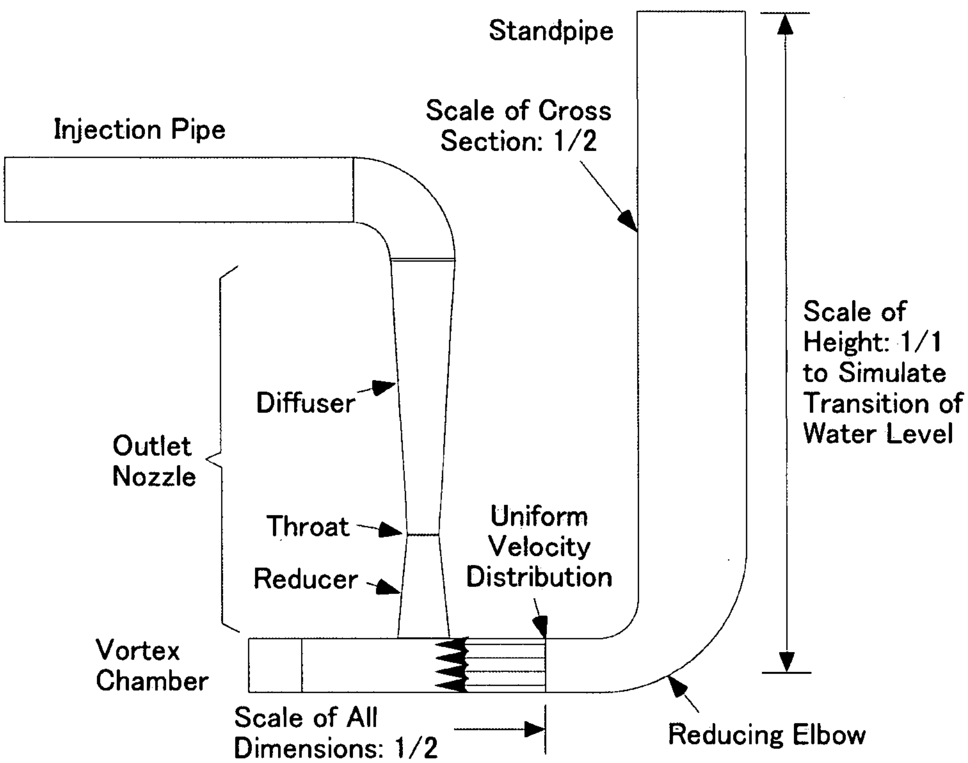

Fig. 36-1 1/2 scale Model of Flow Damper with full-height Standpipe

(a) Generally speaking, the dimensionless groups that represent the important phenomena are the cavitation factor, flow rate coefficient, Reynolds number and Froude number. Their roles are different from each other. Reynolds number represents effect of viscosity on flow resistance. Effect of viscosity is included in the flow rate coefficient which is less dependent on Reynolds number in the plant operating conditions. Since water is isothermal, gravity affects only the boundary conditions at the free surface of water in the accumulator tank and the standpipe, and does not appear in the momentum equation. The cavitation factor directly affects the flow rate coefficient only when cavitation occurs.

(b) As mentioned in Response to RAI 9. UAP-HF-08174-P(R0), the boundary conditions are configurations of the model, inlet condition, namely, gas pressure in the accumulator tank, and outlet condition, namely, outlet pressure of the flow damper for the flow rate coefficient. The characteristic length (D) can be chosen as an arbitrary dimension except the heights of the standpipe and the accumulator tank. Then, the scale is 1/2 for all directions as shown in Fig. 36-1. The flow rate coefficient represents effects of the geometry and viscosity. The former is independent of Reynolds number, and constant for the flow damper with a given configuration for different size facilities. The latter is represented by Reynolds number which has less effect on the flow rate coefficient.

(c) Yes, the response for RAI 9-B (Sept, 2008) is applicable to both large and small flow conditions as mentioned above. Even in case of gaseous cavitation, effect of cavitation is evaluated in cavitation factor taken by the experiments. That is because local pressure is kept at vapor pressure where cavitation occurs. This effect reflects on cavitation factor.

(d) Please see the Response to RAI 33 for the effect of nitrogen on cavitation. If injection starts, cavitation nuclei rapidly grow as pressure decreases in the accumulator tank. The superficial density of water will be degraded only by pressure drop, which is independent of the scale of an accumulator.

RAI 37.

In MHI's response to RAI 10 (Sept 2008) to show similarity of the non-dimensional groups between the ½ scale test and the plant:

(a) What is the basis of assuming that reference velocities in the model and prototype will be equal (Um=Up)?

(b) Is it assumed that the losses in the flow path are preserved?

(c) What is basis of Eq. 10-9?

(d) What is scaloffing?

(e) Why is Cv for model and prototype in Eq. 10-11 the same?

(f) What is the basis for Eqs. 10-12 and 10-13?

Response

(a) Pressures in the accumulator tank and injection line and pressure difference across the flow damper of the full height 1/2 scale model were set to be equal to those of the actual accumulator. The friction of the flow damper is negligible, and form resistance is dominant as mentioned in the response to RAI 9 in this document. The configuration of the model was similar to those of the actual accumulator. Consequently, the velocity will be equal ($Um=U_p$).

(b) As mentioned above, the losses in the flow path will be preserved.

(c) During flow switching, motion of water column in the standpipe obeys the momentum equation, (18-1), cited in the response to RAI 18, UAP-HF-08174-P(R0). Making this equation in a dimensionless form yields a dimensionless parameter that is Eq. 10-9.

(d) The word "scaloffing" should be "scaling." It was mistyped. We apologize for it.

(e) Since friction loss is negligible and form resistance is dominant in the flow damper, Cv must be common both for model and prototype in Eq. 10-11.

(f) The data in Chapter 4.3 of the Topical Report shows flow rate coefficient is common both for 1/5 and 1/2 scale models. Then, it is also true for larger flow damper because of higher Reynolds number. This leads us to the conclusion that $C_{vm} = C_{vp}$ for $\sigma_{vm} = \sigma_{vp}$ both for large and small flow injections. Cavitation factor is an independent variable of the flow damper to get flow rate coefficient, and we can choose $\sigma_{vm} = \sigma_{vp}$.

RAI 38.
Table 11-1 in MHI's response to RAI 11 (Sept 2008) provides a comparison of various dimensions of the flow damper in the actual accumulator, and the 1/2 and 1/5 scaled models. MHI's response to RAI 14 (Sept 2008) stated that the flow rate coefficient depends on ratio of height to diameter for vortex damper, and that most of the energy loss depends on flow in vortex chamber but occurs in the injection pipe.

(a) What scaling rule is applied for determining vortex chamber height?

(b) What is the basis of claim that flow rate coefficient depends on ratio of height to diameter for vortex damper?

(c) Provide any quantitative estimate of losses in vortex chamber and the injection pipe.

Response
(a) The configuration of a model flow damper should be similar to that of an actual flow damper. If configuration of a model is modified, the characteristics of flow rate coefficient with respect to cavitation factor must be divagated from original one.

(b) The height is one of the very important dimensions of the vortex chamber. To understand its role, the flow structure in the chamber during small flow injection is explained first. If fluid were inviscid, there were no velocity boundary layers on the two disk walls of the chamber, then, two-dimensional vortex flow would appear in it. However, real viscous water generates velocity boundary layers on the two disk walls where centrifugal force is weaken and radially inward velocity is formed larger than that out of the boundary layers, or in the main flow where centrifugal force is preserved. Therefore, the height of the chamber determines the ratio of flow rate in the main flow with respect to that in the boundary layers. If the height becomes larger, the rate of the main flow will increase at the same velocity condition. If the thickness of the boundary layers is very small for large Reynolds number, the flow rate in the main flow will be dominant and dependency of flow rate ratio on Reynolds number can be negligibly small. But if the height of the chamber becomes further large for a given flow rate, tangential velocity from the small flow pipe reduces, and centrifugal force of a vortex in the chamber will be weaken. It will degrade the resistance of the flow damper. There is best height between them that is experimentally confirmed so that flow rate coefficients are common for 1/5 and 1/2 scale models and sufficient for the design requirement.

(c) Please see Response to RAI 53.

RAI 39.
Referring to MHI's response to RAI 12 and 13 (Sept 2008):

(a) How is the frictional pressure drop preserved in different scale facilities?

(b) How much of the total pressure drop is contributed by the pressure drop in the vortex chamber?

(c) Is the flow field in vortex chamber controlled by the Reynolds number as defined in topical report MUAP-07001?

Response
(a) Please see Response to RAI 38(b).

(b) Please see Response to RAI 53.

(c) Generally speaking, the flow field in vortex chamber is controlled by the Reynolds number, and effect of viscosity on flow field decrease as Reynolds number goes large. Consequently, experimental investigation is necessary for the evaluation of effect of viscosity on the characteristics of flow rate coefficient of the flow damper.

RAI 40.

MHI's response to RAI 15 (Sept. 2008) regarding the characteristic length in the Froude Number is not clear. The hydraulic diameter of the stand pipe inner section varies with the scale size:[ ]mm, [ ]mm, and [ ]mm for the actual ACC, 1/2 scale and 1/5 scale test facilities, respectively. Therefore, L/d is not preserved.

(a) What length scale is the Froude numbers based on and why?

(b) What is its impact on the flow field?

Response

(a) Please see Response to RAI 36. The data of flow switching taken with 1/5 scale test were not presented in the topical report. The height should be used as a characteristic length for the Froude number. The flow in the standpipe is one-dimensional, and diameters of the models do not affect the transition of water level in the standpipes.

(b) As mentioned above, flow in the standpipe is one-dimensional, and there is no impact of the diameter of the standpipe on the flow field.

RAI 41.

With respect to the uncertainties associated with the accumulator flow characteristic equations, instrumentation, manufacturing, and the flow rate switching water level:

(a) What contributes to bias (systematic) and standard deviation (precision or random) part of uncertainty in the flow rate coefficients of the large- and small-flow characteristic correlations of the flow damper?

(b) What are the other contributors to uncertainty beside instrument uncertainty, dispersion or regression analyses error and manufacturing uncertainties? How are these combined?

(c) What is the relationship between the diversion of correlations listed in Table 3.5-5 (in MUAP-07011 Large-Break LOCA Methodology) and listed in Table 5.2-1 in MUAP-07001)?

Response

(a) Contributors to bias and random part are as follows:

Bias part

1) To measuring uncertainty:
   - Test tank diameter
   - Specific weight of water
   - Height of injection pipe
   - Injection pipe diameter
2) To manufacturing errors
   - Manufacturing tolerance
3) To uncertainty of water level for switching flow rates
   - Level instrument error (guaranteed value by vender)

Random part

1) To measuring uncertainty:
   - Test tank diameter
   - Water Level in Test Tank
   - Pressure drop (pressure loss)
   - Height of injection pipe
   - Injection pipe diameter
2) To experimental equation
   - Dispersion of experimental equation and test data
3) To uncertainty of water level for switching flow rates
   - Deviation between flow switching level and standpipe inlet level

(b) There is no other possible uncertainty. The combinations of uncertainties described above are shown in Reference 41-1, Section 3.5.1.4, item (1), Total Uncertainty of Experimental Equation Applicable to US-APWR (Page 3-27, and 28).

(c) The values in Table 5.2-1 (MUAP-07001) shows dispersion of the test data from experimental equations in each test case (Case 1, 2, 3, 4, and 6). The values in Table 3.5-5 (MUAP-07011, Large-Break LOCA Methodology) shows dispersion of the test data bounding all of Case 1, 2, 3, 4, and 6, from experimental equations. Experimental equations are developed for all of experimental data bounding Case 1, 2, 3, 4, and 6, thus values shown in Table 3.5-5 are used for estimation of experimental equations uncertainty in LOCA analyses.

Reference

41-1 "Large Break LOCA Code Applicability Report for US-APWR", MUAP-07011-P(R0), July 2007

RAI 42.

In MHI's responses to RAI 17 (July 2007) related to instrumentation uncertainties:

(a) How are the bias limits for the six parameters estimated?

(b) Why the biases are zero for the accumulator tank water level, pressure drop and flow rate (Tables 17-1 and 17-2)?

Response

(a) The following is the detailed description of how bias limits of 6 parameters (i.e., test tank diameter, specific weight of water, flow rate, height of injection pipe, injection pipe diameter, flow rate coefficient) are obtained:

1) Test tank diameter: A half of minimum scale value of slide gauge is used as bias limit for test tank diameter. (Reference 42-1, page 32, response 3), (1) to question 17-B.)
2) Specific weight of water: The guaranteed value for instrument accuracy of thermocouple provided by manufacturer is[ ]°C. Temperature difference of[ ]°C corresponds to density difference of[ ]kg/m^3 at normal temperature and pressure. Thermocouples have characteristic bias of [ ]°C, thus this value is treated as the bias limit. Note that the effect of pressure instrument error was neglected since the sensitivity of density is very small as compared with pressure gauge error. (Reference 42-1, page 33, response 3), (3) to question 17-B.)
3) Flow rate: As a relative bias limit, it was calculated from (B_Q/Q) in the 1st. equation in response 5) to question 17-B. (Reference 42-1, page 34.)
4) Height of injection pipe: Please see Reference 42-1, page 33, response 3), (5) to question 17-B.
5) Injection pipe diameter: Bias limit is[ ]mm, which is a half of minimum scale value of micrometer. (Reference 42-1, page 33, response 3), (6) to question 17-B.)
6) Flow rate coefficient: As a relative bias limit, it was calculated from (B_{cv}/Cv) in the 6th. equation in response 5) to question 17-B. (Reference 42-1, page 35.)

(b) Here is the detailed description of how the deviation of test tank water level, pressure drop, and flow rate is treated:

Test tank water level: Normally, a half of minimum scale value of manometer should be used as a bias limit, however, this value is neglected since this bias limit is very small as compared with precision index. Bias limit is[ ]mm which is a half of minimum scale value of[ ]mm. Averaged value of measurements is[ ]m and relative bias limit is[ ], which is as small as approximately[ ]of relative precision index of[ ]that we neglected this value.

Pressure drop (pressure loss): Bias limit is neglected since it tends to be controlled by random part from the result of comparison of deference measured by pressure transducer in test tank and injection pipe with the method shown in the response 3), (4) to question 17-B, Reference 42-1, page 33.

Flow rate: Bias (bias limit) is considered as described in the response to RAI 42(a).

Reference

42-1 Response to NRC's Questions for Topical Report MUAP-07001-P(R1) The Advance Accumulator, UAP-HF-07086-P(R0), July 2007

RAI 43.

Citing ANSI/ASME PTC19.1-1985 in the response to RAI 17 (July 2007), MHI uses the square-root-sum-of-squares (RSS) method to combine bias with precision (standard deviation) in the uncertainty analysis as shown in Eqs. 17.5 and 17.6. The USNRC staff has accepted the RSS methodology for combining the uncertainties that are random, normally distributed, and independent, whereas the algebraic method is used to combine uncertainties that are not random, not normally distributed, or are dependent.

Provide justification of combining bias with precision (standard deviation) through the RSS method.

Response

Validation of using RSS method is shown as follows:

1) Test tank diameter
   Bias limit is a half of minimum scale value of slide gauge while tank inner diameter is measured value and has dispersion, thus they are independent each other. Although measured value of tank diameter has dispersion, it is measured only 7 times, and therefore, the number of data is not enough to consider that the data shows the normal distribution. Thus, equation (17.5) with the Student t-value is used to obtain 95 % of Coverage. Consequently, using RSS method is valid.

2) Test tank water level
   The deviations between differential pressure transducer and manometer are randomly-generated. It is measured only 9 times, and therefore, the number of data is not enough to consider that the data shows the normal distribution. Thus, equation (17.5) with the Student t-value is used to obtain 95 % of Coverage. Consequently, using RSS method is valid.

3) Specific weight
   Bias limit only is used since the specific weight is determined by guaranteed value of manufactures. Random error is not used.

4) Flow damper pressure loss
   The deviations between the test tank and injection pipe pressure under common static pressure were randomly-generated. Therefore, the error can be treated as random. It is measured only 11 times, and therefore, the number of data is not enough to consider that the data shows the normal distribution. Thus, equation (17.5) with the Student t-value is used to obtain 95 % of Coverage. Consequently, using RSS method is valid.

5) Height of injection pipe
   Bias limit is a half of minimum scale value of slide gauge, while height is measured value and has dispersion, thus they are independent each other. Although measured value of height has dispersion, it is measured only 9 times, and therefore, the number of data is not enough to consider that the data shows the normal distribution. Thus, equation (17.5) with the Student t-value is used to obtain 95 % of Coverage. Consequently, using RSS method is valid.

6) Injection pipe diameter
   Bias limit is a half of minimum scale value of manometer, while injection pipe inner

diameter is measured value and has dispersion, thus they are independent each other. Although measured value of injection pipe diameter has dispersion, it is measured only 8 times, and therefore, the number of data is not enough to consider that the data shows the normal distribution. Thus, equation (17.5) with the Student t-value is used to obtain 95 % of Coverage. Consequently, using RSS method is valid.

7) Flow rate
Bias limit and precision index of flow rate is calculated using bias limits and precision indexes of test tank diameter, test tank water level, and water density. Because it is valid to apply RSS method to test tank diameter, test tank water level, and water density, it is also valid to apply RSS method to flow rate which is calculated by these parameters.

8) Flow coefficient
Bias limit and precision index of flow coefficient is calculated using bias limits and precision indexes of pressure drop, test tank water level, water density, height of injection pipe, flow rate, and injection pipe diameter. Because it is valid to apply RSS method to pressure drop, test tank water level, water density, height of injection pipe, flow rate, and injection pipe diameter, it is also valid to apply RSS method to flow coefficient which is calculated by these parameters.

RAI 44.

Following questions are related RAI 18 (July 2007) for manufacturing uncertainty.

a) Throat diameter uncertainty will have effect on the losses and on the velocity for given pressure drop. Eq. 18.1 does not account for this effect. Explain.

b) What is basis of Equation 18.5 and why is it different from Eq. 18.1?

c) What is basis of Eq. 18.6? What is relationship between vortex chamber diameter and flow rate?

d) In MHI's response to RAI 18-A dated July 20, 2007, the flow rate errors due to manufacturing tolerance of the outlet pipe throat diameter, and vortex chamber diameter (Eqs. 18-5 and 18-7, respectively) during small flow injection appear to be off by a factor of 2 (see Eq. 18.3). Confirm the correctness of Equations 18-3, 18-5 and 18-7.

e) In MHI's response to RAI 18A dated July 20, 2007, it specifies a proprietary value for the effect of the collision angle tolerance as a part of manufacturing tolerance on the flow rate coefficient error of flow damper during large flow injection based on the development test data.

Provide the development test data to show the results.

Response

a) The outlet nozzle of the flow damper is similar to a Venturi tube. Flow rate through a Venturi tube is given by the following equation ("Flow Measurement", ASME PTC19 5; 2004):

$$Q = \frac{CA}{\sqrt{1-(d_0/D)^4}}\sqrt{2\Delta P\rho} \qquad (44\text{-}1)$$

where C is coefficient of discharge, A area of a throat, d_0 diameter of a throat, D diameter of inlet pipe, ΔP differential pressure and ρ density of fluid.

Coefficient of discharge is a constant for Reynolds number larger than 2×10^5.

The manufacturing tolerance of the throat is[ ] and

$$d_0 = [\quad] \qquad (44\text{-}2)$$

The possible error of flow rate via the area of the throat will be within

$$\varepsilon_1 \equiv \frac{Q \pm \Delta Q}{Q} - 1 = \frac{A \pm \Delta A}{A} - 1 = \pm 2 \times \frac{\Delta d_0}{d_0} = \pm 2 \times \left[\quad\right] = [\quad]. \qquad (44\text{-}3)$$

The diameter of inlet pipe is $D = [\quad]$. The possible error of flow rate via the velocity of approach factor, $F = 1/\sqrt{1-(d_0/D)^4}$, will be within

$$\varepsilon_2 \equiv \frac{Q \pm \Delta Q}{Q} - 1 = \frac{\sqrt{1-((d_0 \pm \Delta d_0)/D)^4}}{\sqrt{1-(d_0/D)^4}} - 1 = [\quad] \qquad (44\text{-}4)$$

Consequently, the possible error of flow rate via the velocity of approach factor is very small compared to that via the area of the throat, and neglected. In other words, the sum of these possible errors is within

$$\varepsilon \equiv \sqrt{\varepsilon_1{}^2 + \varepsilon_2{}^2} = \sqrt{[\quad]} = [\quad] \qquad (44\text{-}5)$$

The concept of the Response to RAI 25, Reference 44-2 is same as the above explanation.

b) During small flow injection, pressure loss in the flow damper is caused by generation of vortex. During large flow injection, pressure loss in the flow damper is caused by reducing flow path at throat portion. The difference of this pressure loss generation mechanism is the reason of the difference of equation 18.5 and 18.1.

During small flow injection, free vortex is generated in flow damper vortex chamber, and in this case, pressure drop ΔP is the function of the square of inner diameter ratio (ratio of vortex chamber diameter; D and throat diameter; B).

Let P_T is accumulator pressure, suffix 1 to values of outside of vortex chamber, and suffix 2 to values of throat portion, next equation is derived from Bernoulli equation:

$$P_T = P_1 + \frac{\rho u_1^2}{2} = P_2 + \frac{\rho u_2^2}{2} \qquad (44\text{-}6)$$

Where,

$P_{1,2}$: Static pressure
$u_{1,2}$: Velocity
ρ : Density

At the same time, evaluate velocity with free vortex, assuming that peripheral velocity excels radial velocity, then

$$u_1/u_2=B/D \qquad (44\text{-}7)$$

Pressure drop of flow damper is

$$\Delta P = P_T - P_2 = \frac{\rho u_2^2}{2} = \frac{\rho u_1^2}{2}(D/B)^2 \qquad (44\text{-}8)$$

Let cross-section area of small flow pipe be "a," the flow rate "q" is

$$q = au_1 = aB/D\sqrt{\frac{2(P_T - P_2)}{\rho}} \qquad (44\text{-}9)$$

Therefore, assuming that vortex chamber diameter; D, and cross-section area of small flow pipe; "a" are constant, then, the relation of flow rate error Δq/q and throat diameter error ΔB/B is described by next equation

$$\Delta q/q = \Delta B/B \qquad (44\text{-}10)$$

c) In equation 44-9, assuming that throat diameter; B, and cross-section of small flow pipe; "a" are constant, then the relation of flow rate error Δq/q and vortex chamber diameter error ΔD/D is described by next equation

$$\Delta q/q = \Delta D/D \qquad (44\text{-}11)$$

d) Equation 18.3 (error of throat diameter during large flow injection) and equation 18.7 (error of width of small flow pipe during small flow injection) are both derived from that flow rate is proportional to cross-section area of flow. In equation 18.3, flow rate error $\Delta q/q$ is throat diameter error $\Delta B/B$ with a factor of 2 since the cross-section is proportional to square of throat diameter. For detailed description, please see equation 18-1 and 18-2, Reference 44-1.

In equation 18-7, flow rate error$\Delta q/q$ is equal to error of width of small flow pipe $\Delta B/B$ (without factor of 2). This is because that cross-section area of small flow pipe is product of width and height of small flow pipe and, in this case, cross-section is evaluated assuming the height is constant (fixed). Error of height of small flow pipe is evaluated in equation 18-7 assuming the width is constant.

For equation 18-5, see the response b) above.

e) Flow coefficients of flow damper with 3 types of facing angles[ ] were measured by use of 1/5 scale model test apparatus and results are shown in Figure 44-1.

From Figure 44-1, variations of flow coefficient Cv when the facing angle deviates[ ] from the center value of[ ] are listed in Table 44-1.
[ ] is the average of variation widths of flow coefficient at each cavitation factor shown in Table 44-1.

<u>References</u>

44-1 Response to NRC's Questions for Topical Report MUAP-07001-P(R1) The Advance Accumulator, UAP-HF-07086-P(R0), July 2007

44-2 MHI's Responses to NRC's Requests for Additional Information on Advanced Accumulator for US-APWR Topical Report MUAP-07001-P, Revision 1, UAP-HF-08174-P(R0), September 2008

Table 44-1.Variation of flow coefficient for[ ] shifting of facing angle

Figure 44-1 Effect of Facing Angle on Flow Coefficient

RAI 45.

The uncertainties described in RAI 17 and 18 are for instrument uncertainty and manufacturing uncertainty. There is an additional uncertainty due to regression analyses. These uncertainties will address random part of uncertainty.

Why is there no reference to systematic uncertainty (bias) in flow rate coefficient and cavitation factor?

Response

As described in responses to RAI 41 and 42, bias are also considered in the evaluation of uncertainties as well as random.

RAI 46.

The response to Question 19-C (July 2007) about the use of values in Table 5.3-1 of topical report MUAP-07001 is incomplete. This table documents uncertainty in water level at the time of switching.

Explain how this information is used in the safety analysis.

Response

The uncertainty in the water level to enable the flow switching is considered conservatively in the evaluation of the fuel cladding temperature. In the PCT evaluation, the required function of the advanced accumulator is to fill-up the lower plenum promptly during the refill period, then simultaneously raise the water level in the downcomer. Therefore, it is a conservative treatment qualitatively to shorten the duration of the large flow rate mode of the advanced accumulator. In ASTRUM, the maximum uncertainty in the switching level is assumed to result in the shortest duration of the large flow rate mode.

RAI 47.

In topical report MUAP-07001, Table 5.2-1, "Dispersion of the Data from Experimental Equations," provides the standard deviation of the flow rate coefficient of the large- and small-flow characteristic correlations. These standard deviations are different for different test cases. Tables 5.2-2(1/2) and 5.2-1(2/2), provide the instrumentation uncertainties for the large and small flow conditions, respectively, which are different for different test cases and different injection periods. The Manufacturing Error associated with the flow rate coefficient described in the report uses a bounding value (proprietary).

Describe how these uncertainty values are combined and how they are accounted for in the safety analyses?

Response

The combined value of each uncertainty (instrument, dispersion and manufacturing) based on their relative standard deviations is obtained by the treatment of root mean square (R.M.S). For the detailed basis for the calculation of the combined value of each uncertainty, please refer to the Subsection 3.5.1.4 in Reference 47-1.

Reference

47-1 "Large Break LOCA Code Applicability Report for US-APWR," MUAP-07011-P(R0), Mitsubishi Heavy Industries, Ltd., July 2007.

RAI 48.

MHI's response to RAI 18 (Sept 2008) explains the reason for the variation in the standpipe water level from case to case in the ½ scale tests right after the switch from large flow to small flow phase (Figures 4.2.4 of MUAP-07001) as due to the variation of the velocity in the standpipe right before the switch of flow rate. However, physical arguments have not been presented. In addition, there is a sharp drop in the tank outlet pressure at the time of flow switch that is related to the level in the stand pipe.

(a) Explain this sharp drop in the tank outlet pressure.

(b) Provide a physical argument for the variation in the standpipe water level at the time of switch.

(c) Explain how Eq. 18-1 was obtained, and how it is solved to get the results in the Figure 18-1.

Response

(a) The sharp drop in the outlet pressure of the flow damper is engendered by large diminution of flow rate in the injection pipe. Flow rate plummets down to about 1/5 that before flow switching, and pressure in the exhaust tank is kept constant at the experiments. Consequently, the pressure drop over the injection pipe reduces to about 1/25 that before flow switching. It is why the sharp drop appears in the outlet pressure of the flow damper at flow switching.

(b) At the beginning of flow switching, the standpipe is filled with water at large velocity. Then, the water level in the standpipe decrease with the velocity. Pressure at the outlet of the large flow pipe is equal to the static pressure in the small flow pipe, which is lower than the total pressure in the accumulator tank at the amount determined by the dynamic pressure of the small flow pipe. The static pressure stops the motion of water column in the standpipe as follows:
If the water level in the standpipe reduces below the balance level equivalent to the static pressure, the velocity of the water column decreases and stops. Then, the static pressure pushes the water column back to the balance level, and the flow switching comes to an end.

(c) Water hammer analysis discusses one-dimensional momentum balance of a water column in a pipe. Similar discussion leads us to Equation (18-1) as follows:
Momentum change of the water column is expressed by the term on the left hand side of Equation (18-1). Momentum flowing out from the large flow pipe into the vortex chamber is given by the first term, (a), on the right hand side of Equation (18-1). Gravitational force acting on the water column is given by the second term, (b), on the right hand side, flow resistance of the standpipe and the large flow pipe by the third term, (c), and pressure recovery of small flow by the fourth term, (d). There is no pressure recovery of small flow of the flow damper for US-APWR, and the fourth term, (d), turns to null.
It was solved numerically. Pressure drop in the injection pipe is caused by the large flow resistance of the flow damper, and the pressure in the exhaust tank was kept constant at the tests. So there is no pressure effect to the dynamics of water column in the standpipe.

RAI 49.

MHI's response to RAI 19 (Sept 2008) explains the reason for the peak flow rate variation in magnitude and timing from case to case for the ½ scale tests. It states that in Case 4 the peak flow rate is larger than the Case 1, because Case 4 has higher back pressure despite having a smaller differential pressure. The ΔP in Case 1 (576 psi) is larger than in Case 4 (515 psi) but the peak flow rate is smaller.

(a) Is there larger cavitation (voiding) in Case 1?

(b) What is the cause of larger peak in Case 4? The response does not provide physical reason for this observation.

Response

(a) Yes. Cavitation (voiding) is larger in Case 1. The reason for this is that pressure difference of the flow damper in Case 1 is larger than that in Case 4, and flow damper outlet pressure is smaller than that in Case 4. Please see the cavitation factor when the outlet valve of the test tank becomes fully open in the response to RAI 51.

(b) Peak flow rate appears when the outlet valve of test tank becomes fully open. As described in item (a) above, cavitation (voiding) in Case 4 is smaller, and resistance of flow damper becomes smaller. Therefore, peak flow rate becomes larger though ΔP is smaller.

RAI 50.

MHI's response to RAI 20 (Sept 2008) explains why Case 1 have lower cavitation factors than Case 7 despite having higher pressures for small flow regime. It seems that cavitation factor does not represent any physics related to voiding in these tests. There can be choking in the diffuser section if voiding begins near the throat. In case of such choking, the cavitation factor becomes independent of the injection pipe exit pressure.
What is the purpose of using cavitation factor as one of the parameter?

Response

Cavitation factor is used for large flow injection, but not needed for small flow injection, since there is no effect of cavitation to flow rate coefficient. At the start of the development of the advanced accumulator, little information was available to substantiate the empirical estimation, but the results were later confirmed with experimental data.

There is no choking at the throat of the flow damper both for large and small flow injection as mentioned in Response to RAI 30, and cavitation factor can be used as a parameter for flow rate coefficient.
If there were a cavitation at the throat, it would be incompatible with the facts that minimum pressure will be in the diffuser and that flow rate coefficient is determined only by cavitation factor.

RAI 51.

Referring to MHI's response to RAI 10 (July 2007) and RAI 19 (Sept 2008) regarding the full height, ½ scale test results shown the Figures 4.2.4 in topical report MUAP-07001:
How is the flow damper outlet pressure (P_D) calculated? Where is the device located, and what is its uncertainty? Also, please provide the early pressure, flow rate, and other related data missing from the ½ scale data sheets (Topical Report and July 2007 response). As much as the first 4 seconds are missing in some cases.

Response

The flow damper outlet pressure measured in the tests was reduced to the flow damper outlet pressure P_D based on the as-built scale as follows:

$$P_D + \rho \cdot V_D^2/2 = P_D' + \rho \cdot V_D'^2/2 \quad (51\text{-}1)$$

$$P_D = P_D' + \rho \cdot V_D'^2/2 - \rho \cdot V_D^2/2 \quad (51\text{-}2)$$

$$V_D = V_D' \cdot (D'/D)^2 \quad (51\text{-}2)$$

Where,

- P_D : Static pressure at as-build flow damper outlet piping
- P_D' : Measured static pressure at flow damper outlet piping in test
- V_D : Flow velocity in as-built piping
- V_D' : Flow velocity in test piping
- D : Inner diameter of as-built piping
- D' : Inner diameter of test piping
- ρ : Fluid density

Flow damper outlet pressure was measured by pressure gauges at the injection pipe. Pressure measuring points are shown in Figure 51-1. Instrumental error is{ }of measuring span.

Attachment A to Reference 51-1 shows flow rates, cavitation factors, and flow rate coefficients every one second in Cases 1 to 4, which is response to the requirement of NRC. The provided data start at 4 second.

Because the flow rate widely varied in a short period of time until the test tank outlet valve become fully opened, the data in these periods did not have any meaning for evaluating the characteristics of flow damper.

Therefore, Table 51-1 shows the data just before the first 4 second, where the valve had just fully opened.

The time to full open of the valve became longer if pressure difference of the valve, or pressure difference between the test tank and the backpressure tank, was larger.

Reference
51-1 Response to NRC's Questions for Topical Report MUAP-07001-P(R1) The Advance Accumulator, UAP-HF-07086-P(R0), July 2007

Table 51-1 Full-height 1/2 Scale Test Data

Test Case	Time (sec)	Test tank pres. (kg/cm^2)	Flow damper outlet pres. (kg/cm^2)	Test tank level (m)	Tank water temperature (°C)	Flow rate (m^3/s)	Cavitation factor σ_V	Flow rate coefficient C_V

Figure 51-1 Full Height 1/2 Scale Test Facility Outline Drawing

RAI 52.

In MHI's response to RAI 26 dated September 2008, how was mass flow rate ainty?

Response

The same flow rate calculation method is used for both small and large flow injection as described in the answer to RAI-26 in Reference 52-1. [ ] of uncertainty is expected.

Reference

52-1 MHI's Responses to NRC's Requests for Additional Information on Advanced Accumulator for US-APWR Topical Report MUAP-07001-P, Revision 1, UAP-September 2008

RAI 53.

In the conference call on February 25, 2009, MHI indicated it has performed CFD calculations on the advanced accumulator.

Provide any final report about the CFD calculations, including the case and data files used to make the conclusions about the flow performance map (i.e. flow rate vs. time) as well as cavitation throughout the time of performance of the accumulator during both the large flow rate and small flow rate conditions.

Response

Please see Attachment 1, Flow in the Flow Damper by Computational Analysis.

Attachment A

Flow in the Flow Damper by Computational Analysis

Non Proprietary Version

1. Objectives

We have confirmed the flow in the flow damper with some scale models. In addition to that, we tried to investigate the flow for the models and the prototype for small flow injection using computational fluid dynamics.

2. Method of Computational Fluid Dynamics

Computational Code: Fluent Ver. 6.2.16 developed by Fluent Inc.
Method: Steady State Analysis of Incompressible Viscous Flow
Turbulence Model: RSM (Reynolds Stress Model)
Solid Boundary: Using Wall Function
Discretization: Second-order Accurate Up-Wind Method for Equation of Motion
First-order Accurate Up-Wind Method for the others

3. Analytical Model

It consists of the small flow pipe, the vortex chamber, the outlet nozzle with the throat and the diffuser, and the injection pipe. Lower part of the standpipe was also modeled.

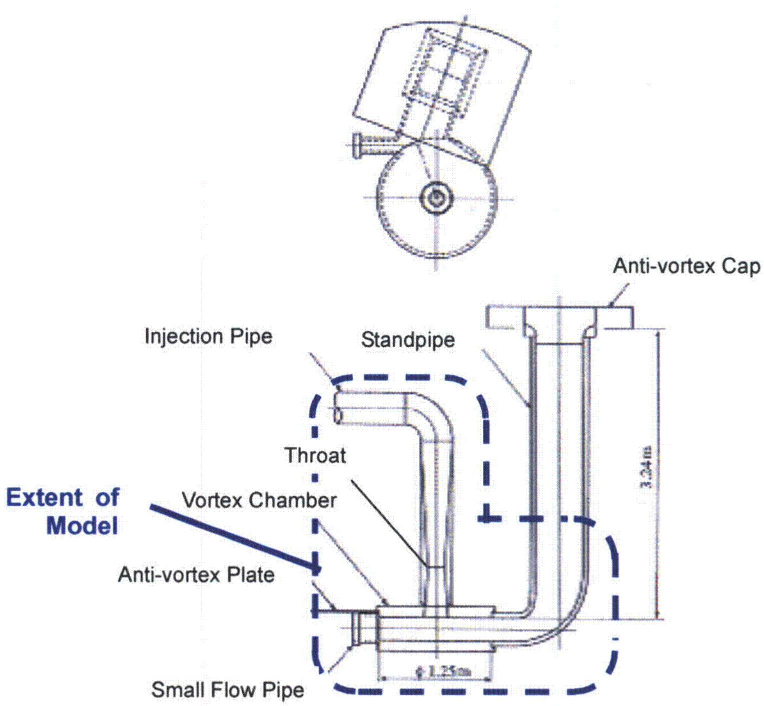

3.5 million Cells

Fig. 1b Computational Model

4. Selected Cases and Models for Calculation

The cavitation factors were $\sigma_V = 0.3$ for the minimum value at the actual plant condition, and $\sigma_V = 9.4$ for the maximum value at the model tests.

The model scales were 1/5, 1/2 and 1/1.

The boundary conditions were from the test conditions of 1/2-scale model.

Table 1 Conditions for the Calculation

Test Case	Case 1	Case 6
Cavitation Factor	0.3	9.4
Inlet Velocity at Small flow Pipe		
Inlet Velocity at Standpipe		
Pressure at Exit of Injection Pipe		

5. Results

5.1 Flow Patterns

Figure 2 shows the flow patterns were similar to each other for 1/5- and 1/2-scale models, and the prototype.

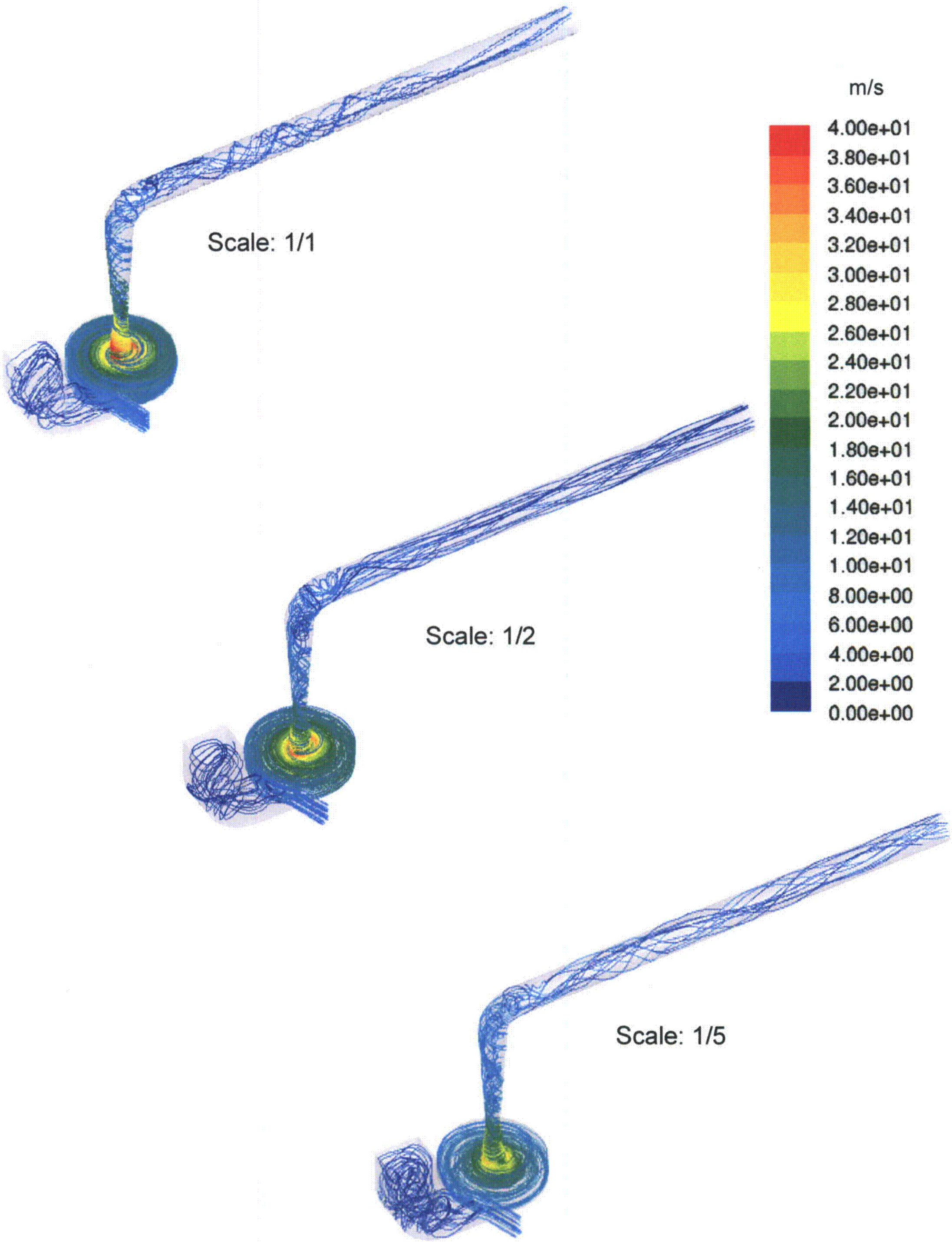

Fig. 2 Flow Patterns for σ_V =0.3

5.2 Total Pressure Distributions

The energy loss from the small and large flow pipes to the throat is about 90% of the total loss for all cases.

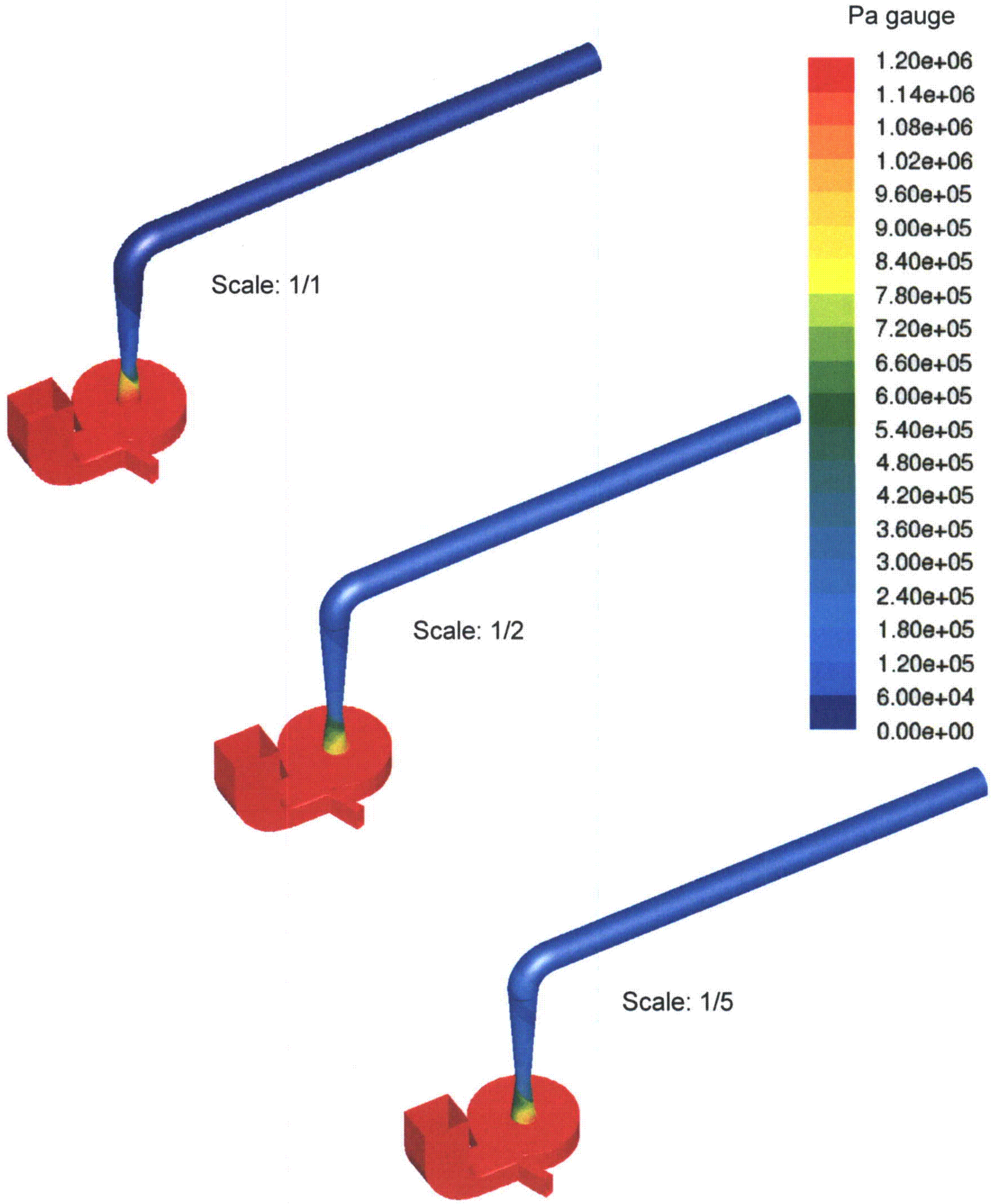

Fig. 3 Total Pressure distribution for σ_V =0.3

5.3 Static Pressure Distributions in Vortex Cambers

The static pressure distributions in the vortex chambers are similar to each other for all cases.

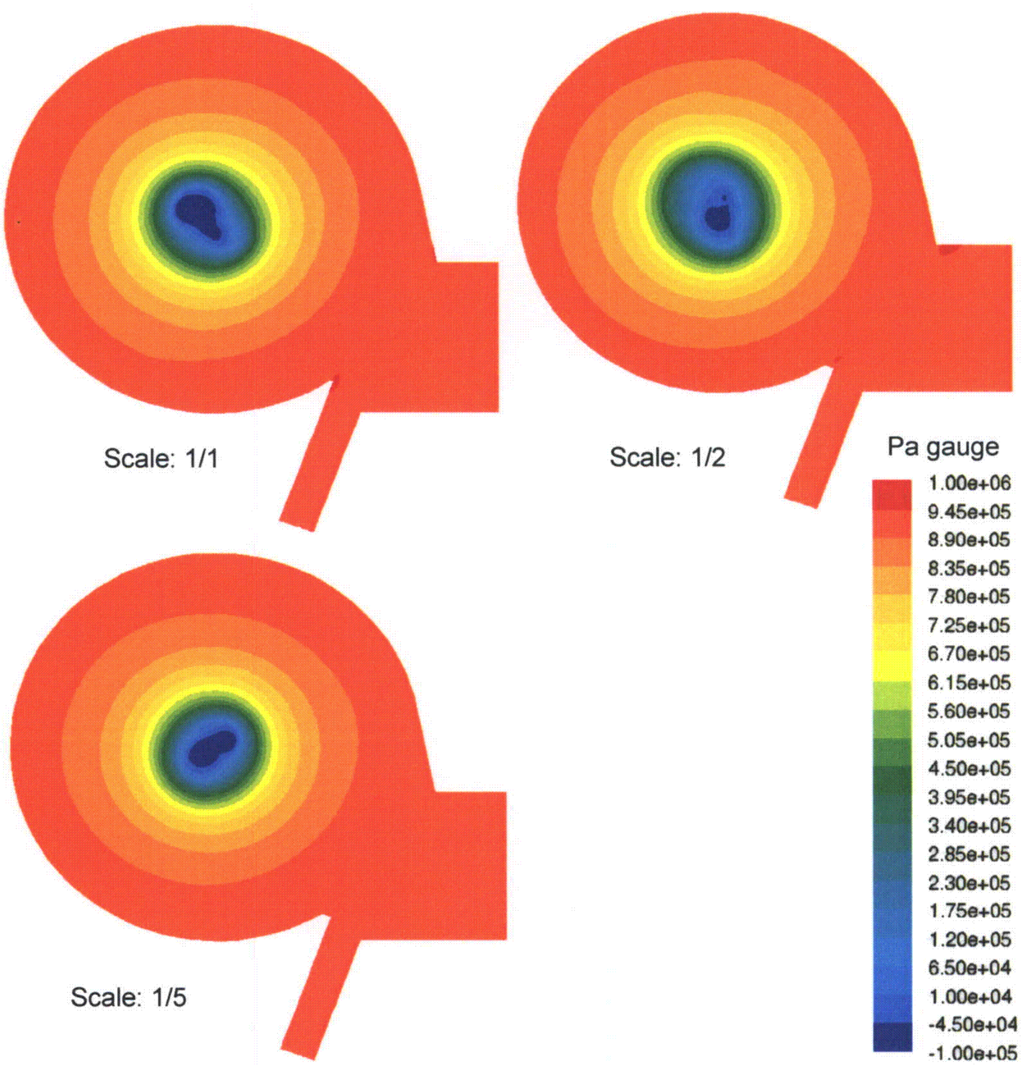

Fig. 4 Static Pressure distribution in Vortex Camber for σ_V =0.3

5.4 Flow Rate Coefficient

Flow rate coefficient is independent of model scale both for cavitation factor σ_V =0.3 and 9.4.

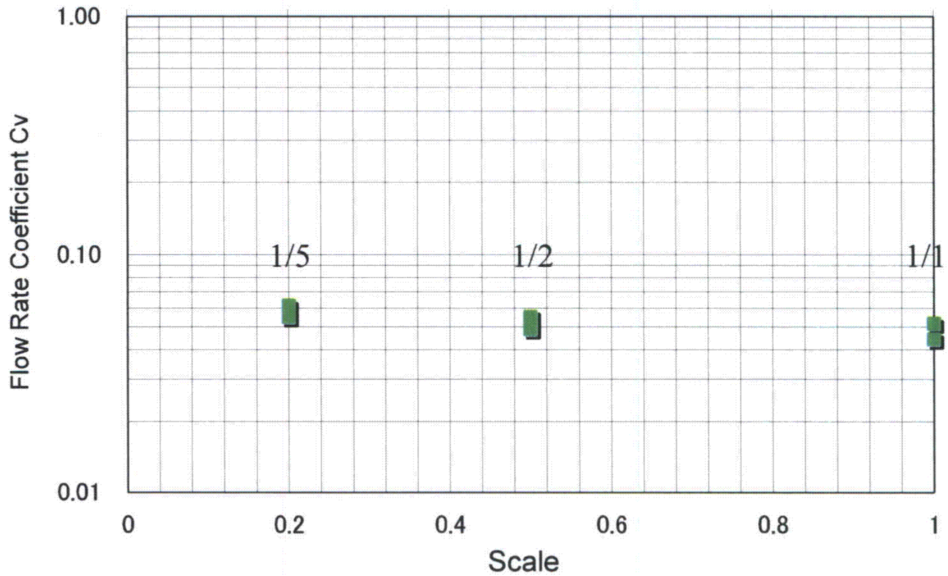

Fig. 4 Flow Rate Coefficient of Flow Damper for σ_V =0.3

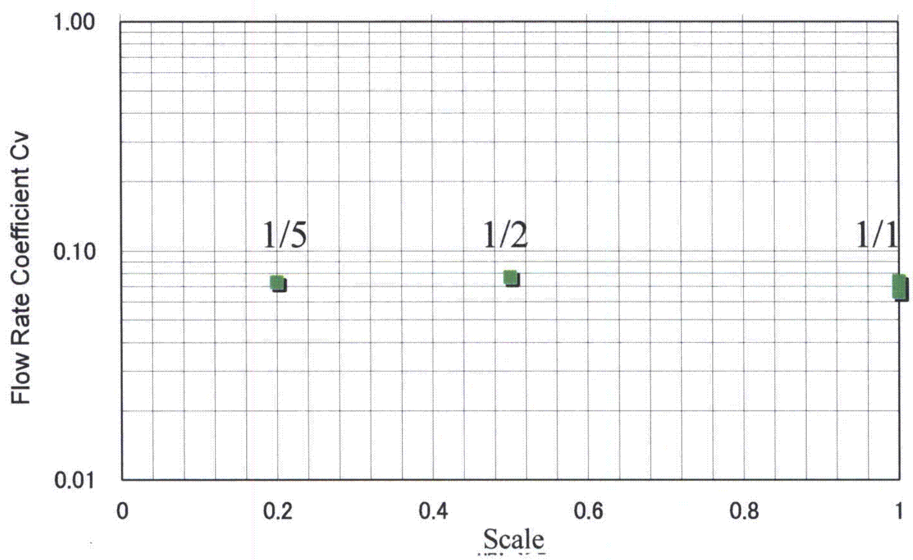

Fig. 5 Flow Rate Coefficient of Flow Damper for σ_V =9.4

5.5 Energy Loss Distribution

The energy loss from the small and large flow pipes to the throat is about 90% of the total loss for all cases of σ_V =0.3.

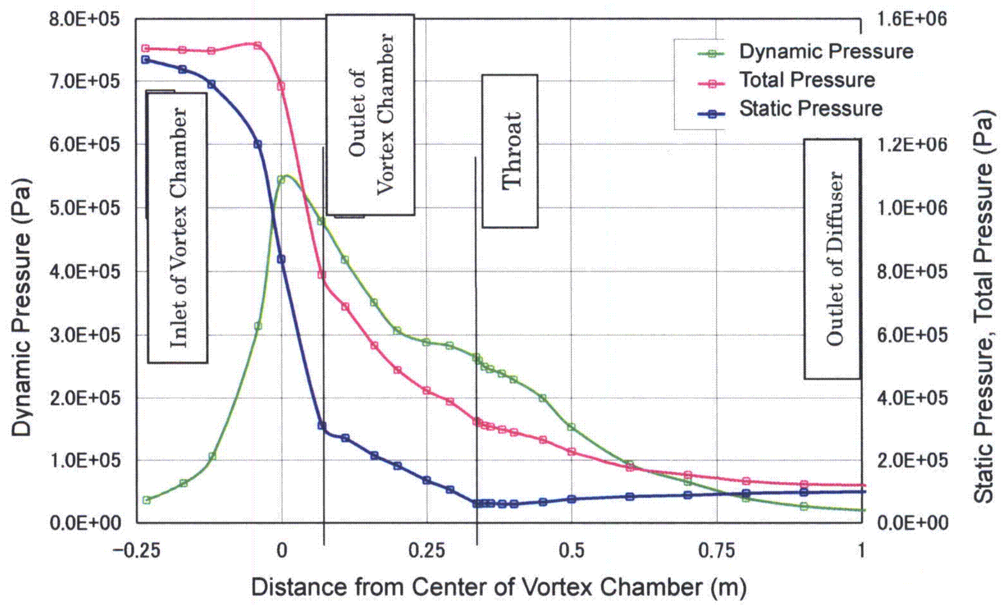

Fig. 6 Example of Pressure Distributions of 1/2-scale Model for σ_V =0.3

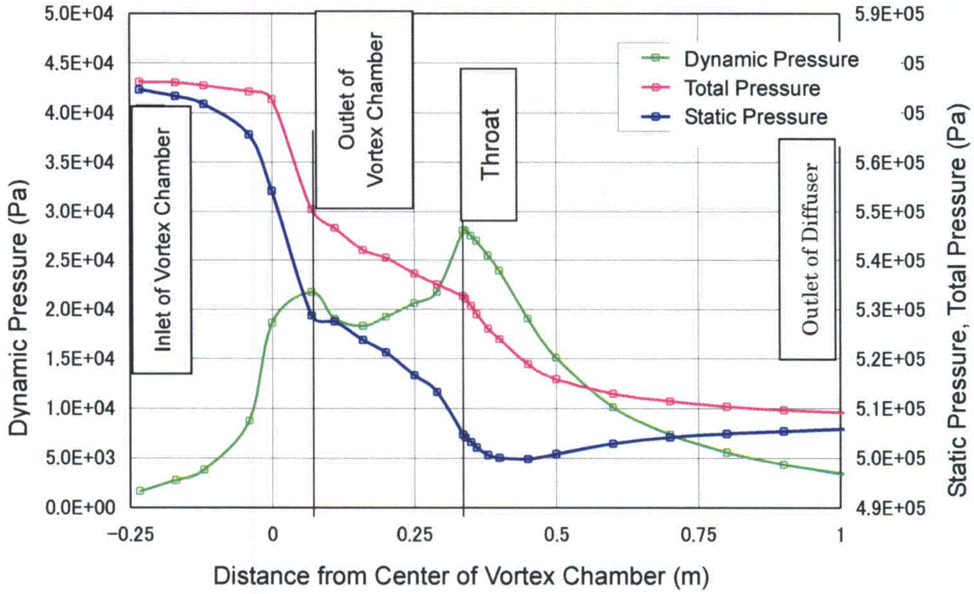

Fig. 7 Example of Pressure Distributions of 1/2-scale Model for σ_V =9.4

5.6 Cavitation

Cavitation may occur in the vortex chamber. Flow path surrounding the cavitation has larger area than that of the throat so that cavitation does not choke the flow rate.

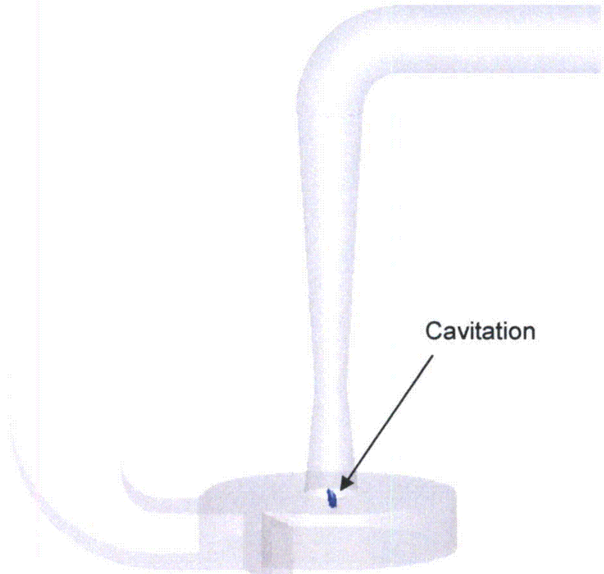

Fig. 8 Cavitation in 1/2-scale Model for σ_V =0.3

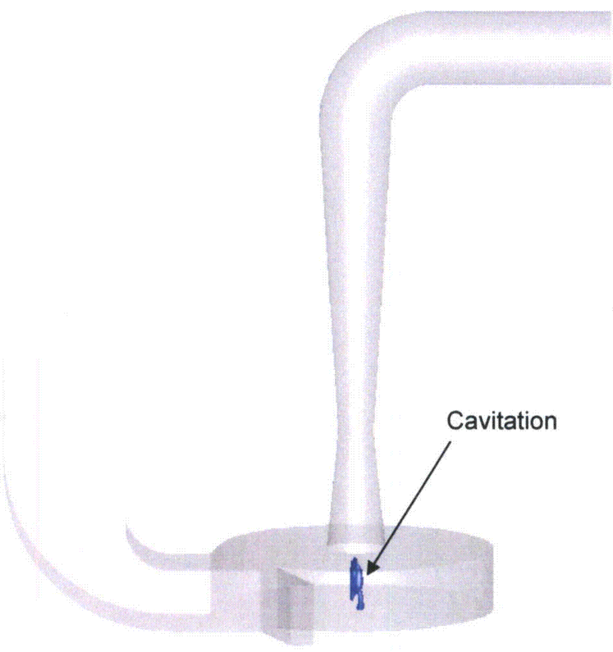

Fig. 9 Cavitation in 1/1-scale Model for σ_V =0.3